

# Temperature of intermediate mass fragments in simulated $^{40}\text{Ca} + ^{40}\text{Ca}$ reactions around the Fermi energies by AMD model

Chun-Wang Ma<sup>1</sup> · Chun-Yuan Qiao<sup>1</sup> · Tian-Tian Ding<sup>1</sup> · Yi-Dan Song<sup>1</sup>

Received: 12 April 2016/Revised: 23 June 2016/Accepted: 1 July 2016/Published online: 26 August 2016

© Shanghai Institute of Applied Physics, Chinese Academy of Sciences, Chinese Nuclear Society, Science Press China and Springer Science+Business Media Singapore 2016

**Abstract** The primary fragments in  $^{40}\text{Ca} + ^{40}\text{Ca}$  reactions at 35, 50, 80, 100, 140, and 300 MeV/u were simulated using the antisymmetrized molecular dynamics model, in the phase space at  $t = 300$  fm/c with a coalescence radius  $R_c = 5$  fm. The standard Gogny interactions g0, g0as, and g0ass were adopted in simulating the collisions at an impact parameter of  $b = 0$  fm. It was found, using an isobaric yield ratio method, that temperature of the primary fragment depends on the incident energy and hardness of the interaction potential. The temperature obtained in this work agrees with the results by the self-consistent fitting method.

**Keywords** Temperature · Isobaric yield ratio · Intermediate mass fragment · Heavy-ion collisions

## 1 Introduction

Temperature is important in heavy-ion collisions, which increases rapidly with the colliding time to reach the maximum and then decreases due to cooling down of the colliding system in expansion [1]. The methods for studying the temperature in heavy-ion collisions above the

Fermi energy include the double isotopic ratio (Albergo thermometer) of the light particles/fragments [2], the thermal energy method [3], the excitation energy method [4], the momentum fluctuation method [5], and the slope temperature using the kinetic energy spectra of light particles [6]. Being mostly focused on the extraction of temperature from light particles, the methods for temperature are correlated with each other [1, 7]. Another method is the intermediate mass fragments (IMFs). Assuming the colliding system to be in an equilibrium state, and using the Albergo temperature to extract temperature, the isotopes of carbon and the heavier [8, 9] were found to carry a much lower temperature than the light particles, because that the fragments and the light particles denote the different colliding times and the light particles are emitted earlier than the fragments. The isobaric yield ratio (IYR) was used to determine the temperature for IMFs in the framework of the thermodynamics models, and different methods were used to approximate the free energy of IMFs [10–13]. This isobaric yield ratio method has been improved by adopting the difference between two IYRs and avoiding the fitting procedure to IYR, so as to obtain the temperature directly from the isobaric yields [14]. Liu et al. [15–17] developed an isobaric yield ratio method using the symmetry energy of primary fragment and the prefixed symmetry energy of the source in which the primary fragments are formed (the primary fragments mean that they are formed in the colliding source, which are highly excited and will undergo the secondary decay to form the final fragments). The temperature of fragments is determined at the formation time in a self-consistent manner. In their works, the fragments in the  $^{40}\text{Ca} + ^{40}\text{Ca}$  reactions were simulated using the antisymmetrized molecular dynamics (AMD) model [15]. In Ref. [10], a similar method was used to determine

This work is supported by the Program for Science and Technology Innovation Talents in Universities of Henan Province (13HASTIT046), Henan Normal University for the Excellent Youth (154100510007). Yi-Dan Song thanks the support from the Creative Experimental Project of National Undergraduate Students (CEPNU 201510476017).

✉ Chun-Wang Ma  
machunwang@126.com

<sup>1</sup> Institute of Particle and Nuclear Physics, Henan Normal University, Xinxiang 453007, China

the temperature for IMF by taking the symmetry energy coefficient ( $a_{\text{sym}}$ ) of ground state nucleus as the reference. Due to the strong mass dependence of  $a_{\text{sym}}$  in isobars, the temperature strongly depends on mass. It is interesting to see if the temperature determined by the method in Ref. [10] is similar to those in Refs. [15–17]. In this article, the IYR methods to determine the temperature are described in Sect. 2. The temperature obtained from the simulated fragments using the AMD model is discussed in Sect. 3. A summary of this article is given in Sect. 4.

## 2 Methods

In this work, we call the nucleus produced in collisions as a fragment, which has temperature. And we call the nucleus in its ground state as nucleus to differ it from the fragment. The methods to obtain the ratio of  $a_{\text{sym}}/T$  for IMFs are similar to that developed by Huang et al. [18]. In this article, the IYR method in Ref. [10] is adopted to obtain  $a_{\text{sym}}/T$  for the primary IMF in the framework of the modified Fisher model (MFM) [18–21],

$$a_{\text{sym}}^*/(AT) = [\ln R(I, I-2, A) - \ln R(I+2, I, A) + \Delta E_C - \Delta_{I-2} + \Delta_I]/2, \quad (1)$$

where  $a_{\text{sym}}^* = 4a'_{\text{sym}}$  and the prime denotes the fragment;  $R$  is the yield ratio between isobars differing 2 in  $I$  ( $I = N - Z$ );  $\Delta E_C$  is the residue Coulomb energy, which can be omitted [22];  $\Delta_{I-2}$  and  $\Delta_I$  are the mixing term of  $N$  and  $Z$  of the isobars.

$a_{\text{sym}}$  of nucleus is obtained from the binding energy [27],  $a_{\text{sym}}^*/A = [B(I) - B(I+2) + \Delta E_C]/(I+1)$ , (2)

where  $a_{\text{sym}}^* = 4a_{\text{sym}}$  and  $B$  is the binding energy.  $T$  is determined from the ratio of Eq. (2) to Eq. (1),

$$T = \left( a_{\text{sym}}^*/A \right) / \left[ a_{\text{sym}}^*/(AT) \right]. \quad (3)$$

Similar ratio form of Eq. (3) is used to determine  $T$  for the primary IMFs, with each nucleus having a different  $a_{\text{sym}}^*/A$  [10], while it is the same for the primary IMFs in the self-consistent fitting method and is prefixed in simulations [15].

We note that the coefficients of energy terms contributing to the free energy of fragment depend on both nuclear density ( $\rho$ ) and temperature [18–21], i.e.,  $a_{\text{sym}}^* = a_{\text{sym}}^*(\rho, T)$ . It is shown that the  $\rho$  and  $T$  dependence of  $a_{\text{sym}}^*/(AT)$  can be determined from the correlation between  $a_{\text{sym}}^*/(AT)$  and  $T$  by introducing a  $T$ -dependent symmetry energy [10]. If the coefficients and temperature are free parameters in the modified Fisher model, they can be fitted from the fragment distributions [26].

## 3 Results and discussion

The  $^{40}\text{Ca} + ^{40}\text{Ca}$  reactions at  $E = 35, 50, 80, 100, 140,$  and  $300$  MeV/u were simulated using the AMD model by Liu et al. [15]. The yields of primary fragments were extracted, and the temperature was investigated using the self-consistent fitting method. In this paper, the same yields of primary fragments are used to analyze the temperature according to Eq. (3). In the simulations and the primary fragment reorganizations in Ref. [15], we use three standard Gogny interactions [24] ranging from the soft g0 [24], the hard g0as [25] to the super-hard g0ass interaction [15, 25]. The impact parameter is set as  $b = 0$  fm to simulate the central collisions. Over 10,000 events are simulated for different reactions and Gogny interactions. The fragments are recognized in the phase space at  $t = 300$  fm/c with a coalescence radius  $R_c = 5$  fm [15].

In Fig. 1,  $a_{\text{sym}}^*/(AT)$  for IMF and  $a_{\text{sym}}^*/A$  for nucleus are plotted, with the fragments being  $A \leq 30$ . The AME12 binding energy of nucleus was adopted to obtain  $a_{\text{sym}}^*/A$  [28]. Only the results for  $I = 1$  fragments are shown. It can be seen that both  $a_{\text{sym}}^*/(AT)$  and  $a_{\text{sym}}^*/A$  decrease with increasing  $A$ . The odd–even staggering is more obvious in  $a_{\text{sym}}^*/A$  than in  $a_{\text{sym}}^*/(AT)$ , indicating that the symmetry energy obtained from the primary fragment is smaller than that from the ground state nucleus. This is because that the temperature increase results in a decrease in symmetry energy [29]. The  $a_{\text{sym}}^*/(AT)$  for IMF decreases in an order of the g0, g0as, and g0ass potentials, with the g0as and g0ass results being of a small difference.

As shown in Fig. 2,  $T$  for IMFs calculated by Eq. (3) does not change much at 35 and 50 MeV/u, while it varies with  $A$  at  $E \geq 80$  MeV/u, especially for the IMFs of  $A > 20$ . In a reaction of certain incident energy,  $T$  increases with the interaction in an order of g0, g0as, and g0ass, indicating that  $T$  increases with the hardness of interaction. In super-hard g0ass interaction,  $T$  for IMFs changes greatly with  $A$  at  $E \geq 80$  MeV/u. These phenomena reflect the change of  $a_{\text{sym}}^*/(AT)$  for fragments in reactions of different reactions, induced by the change in yield of fragments. Our results are close to  $T$  obtained by the self-consistent fitting method (lines in Fig. 2) in Ref. [15]. Since the primary IMFs are all reorganized at  $t = 300$  fm/c in the reactions of different incident energies, suggesting that in reaction of relative low incident energies, the primary IMF may easily reach thermal equilibrium, while the trend changes at higher incident energies, where the Pauli blocking is less effective and the symmetry potential is less important, thus leading to a shorter momentum relaxation time and a longer isospin relaxation time [23]. An  $A$ -dependence of temperature was found in measuring fragments in the  $1A \text{ GeV } ^{124,136}\text{Xe} + \text{Pb}$  reactions [10] and in other isobaric

**Fig. 1**  $a_{\text{sym}}^*/(AT)$  calculated by Eq. (1) for the primary IMF in the  $^{40}\text{Ca} + ^{40}\text{Ca}$  reactions at 35, 50, 80, 100, 140, and 300 MeV/u by the AMD model with the g0, g0as, and g0ass interactions, and  $a_{\text{sym}}^*/A$  for nucleus (squares) calculated by Eq. (2)

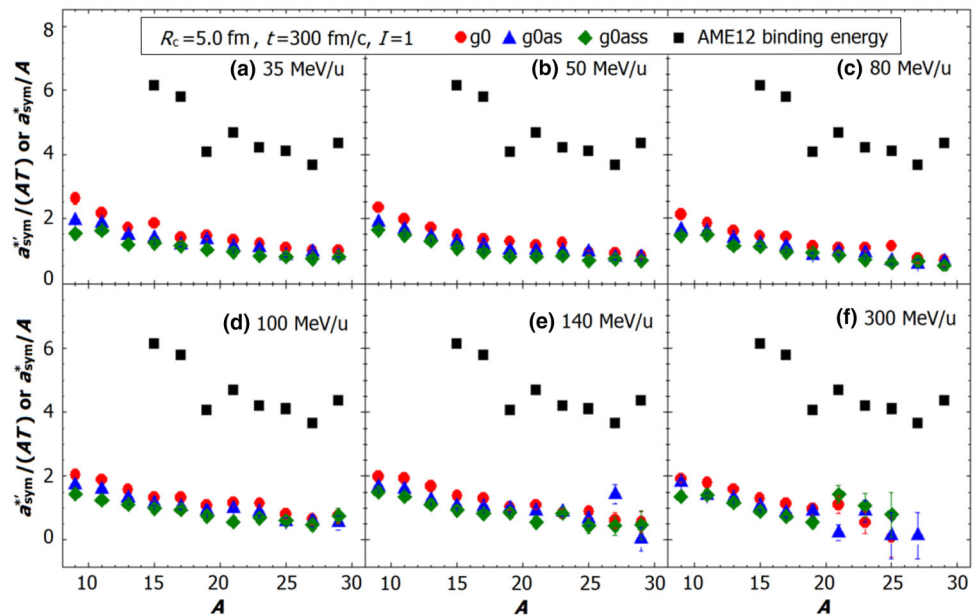
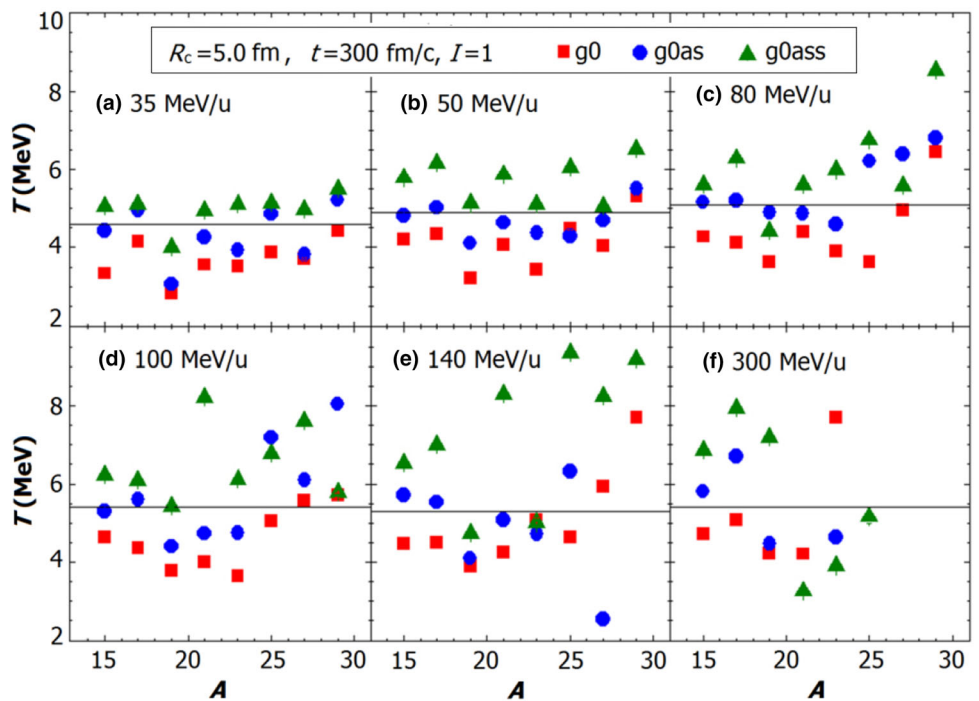


**Fig. 2**  $T$  calculated using Eq. (3) for  $I = 1$  primary IMFs in  $^{40}\text{Ca} + ^{40}\text{Ca}$  reactions simulated at different energies by the AMD model with the g0, g0as, and g0ass interactions. The line in each panel denotes the results of the self-consistent temperature in Ref. [15]



yield ratio methods with simulated primary fragments [15] or measured cold fragments [14]. The  $A$ -dependence of temperature has been explained as effects of the finite reaction system [15]. After the self-consistent fitting procedure, the temperature for the primary fragments is almost the same, while after modification by the secondary decay of the primary fragments, the temperature for the resultant cold fragments depends significantly on  $A$ . This is because

that for the cold fragment, its free energy can be approximated by its binding energy at low temperatures.

Figure 3 shows  $T$  for fragments of  $A = 15, 17,$  and  $19$  in reactions simulated using the g0, g0as, and g0ass interactions. Although staggering can be seen in the g0ass, results generally increase with  $E$ , in an order of the g0, g0as, and g0ass, indicating that the harder the interaction the higher temperature of IMFs. This disagrees with the results in

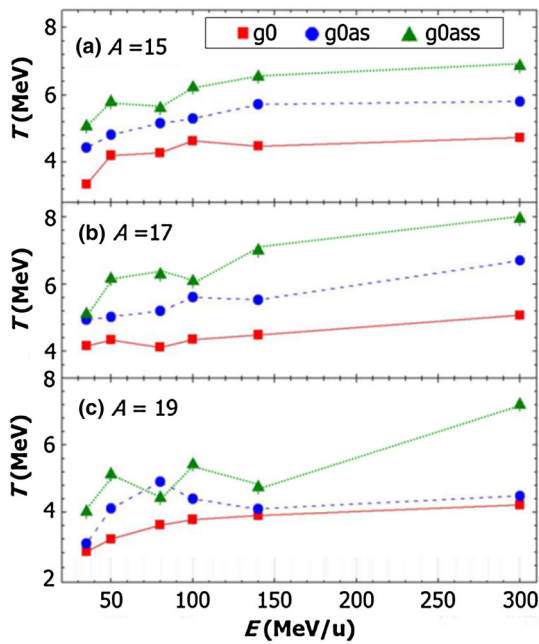
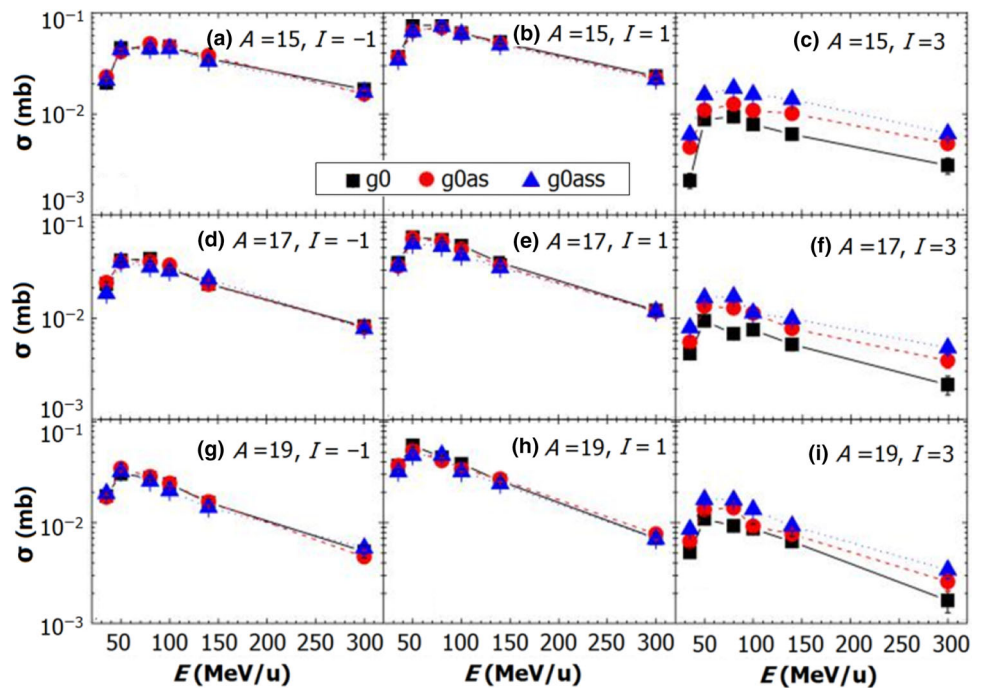


**Fig. 3** Correlation between  $T$  and  $E$  of the reactions for the  $A = 15, 17$ , and  $19$  fragments with  $I = 1$

Ref. [15], where the temperature is insensitive to the interactions, while in our method  $T$  is sensitive to IYR or the cross section of fragment.

Staggering was found in  $T$  for reactions at around 100 MeV/u. Cross sections of the related isobars are plotted in Fig. 4. For  $I = -1$  and  $I = 1$  isobars, the interactions affect little the cross sections, while for  $I = 3$  isobars,

**Fig. 4** Cross sections of the simulated fragments in calculating temperature of the  $A = 15, 17$ , and  $19$  isobars shown in Fig. 3



the interactions affect greatly the cross sections, with obvious staggering. The staggering in  $T$ , or  $a_{\text{sym}}^{*l}/(AT)$ , is due to the staggering of cross sections of the  $I = 3$  isobars, i.e., in the isobaric ratio method the temperature is vulnerable to the change of cross sections of fragments which are influenced by the incident energy, the interaction, and the nucleus–nucleus cross sections, etc.

At last, it should be noted that  $a_{\text{sym}}^{*l}/(AT)$  for fragment is influenced by IYRs and the cross sections of fragments [19]. It has been shown that  $T$  for the measured fragments in the  $^{124,136}\text{Xe}$  reactions are similar, indicating that the temperature tends to be similar in reactions of similar environments [10]. In fact, the results of  $a_{\text{sym}}^{*l}/(AT)$  for fragments reflect the properties of the nuclear system at the time they are generated, which is reflected by different types of the Gogny interactions we used. One would like to expect that  $R_c$  affects the temperature in this isobaric method since it definitely affects the yield of fragment. We cannot perform the analysis for the primary fragments reorganized using different  $R_c$  due to difficulties in obtaining the data, but it can be assumed that the  $R_c$  effect on the temperature in this method shall be small. The reason is that the primary fragments are formed in similar colliding source and the fragments can be viewed as the samples of the source. And the samples of different sizes shall deliver the similar information of the source.

One question frequently raised is whether the equilibrium state can be achieved in the transport model simulations. Liu et al. [15] proposed that the AMD simulations should have a freeze out stage, which is a common concept

of statistical theory. The Shannon information entropy theory has been introduced to study the complex evolution of heavy-ion collision, which can bridge the results in the transport models and thermal dynamics models [30, 31]. It will be interesting to study the temperature evolution in the simulated reactions by the AMD model using the information entropy method.

## 4 Conclusion

Temperature of the primary IMF in simulated  $^{40}\text{Ca} + ^{40}\text{Ca}$  reactions at 35, 50, 80, 100, 140, and 300 MeV/u by the AMD model adopting the standard Gogny  $g_0$ ,  $g_0\text{as}$ , and  $g_0\text{ass}$  interactions [15] has been determined using the IYR method. The primary fragments are reorganized in the phase space at  $t = 300$  fm/c with the coalescence radius  $R_c = 5.0$  fm.

The  $a_{\text{sym}}^*/(AT)$  for the primary fragments simulated by the AMD model is obtained from the difference in IYRs, and  $a_{\text{sym}}^*/A$  for nucleus is determined from the difference between the binding energies of isobars.  $T$  for the primary fragment is determined from the ratio of  $a_{\text{sym}}^*/(AT)$  to  $a_{\text{sym}}^*/A$ .  $T$  increases with the incident energy and the interaction hardness. The temperature we obtained is close to those determined by self-consistent method. The data of primary fragments in the simulated reactions are useful.

**Acknowledgments** We thank Dr. Xing-Quan Liu for sharing their simulated data of the  $^{40}\text{Ca} + ^{40}\text{Ca}$  reactions by the AMD model with us.

## References

1. J. Wang, R. Wada, T. Keutgen et al., Tracing the evolution of temperature in near Fermi energy heavy ion collisions. *Phys. Rev. C* **72**, 024603 (2005). doi:10.1103/PhysRevC.72.024603
2. S. Albergo, S. Costa, E. Costanzo et al., Temperature and free-nucleon densities of nuclear matter exploding into light clusters in heavy-ion collisions. II *Nuovo Cimento A* **89**, 1–28 (1985). doi:10.1007/BF02773614
3. H. Zheng, A. Bonasera, Density and temperature of fermions from quantum fluctuations. *Phys. Lett. B* **696**, 178–181 (2011). doi:10.1016/j.physletb.2010.12.019
4. D.J. Morrissey, W. Benenson, E. Kashy et al., Excited state production and temperature measurement in a heavy ion reaction. *Phys. Lett. B* **148**, 423–427 (1984). doi:10.1016/0370-2693(84)90730-5
5. S. Wuenschel, A. Bonasera, L.W. May et al., Measuring the temperature of hot nuclear fragments. *Nucl. Phys. A* **843**, 1–13 (2010). doi:10.1016/j.nuclphysa.2010.04.013
6. G.D. Westfall, B.V. Jacak, N. Anantaraman et al., Energy dependence of nuclear matter disassembly in heavy ion collisions. *Phys. Lett. B* **116**, 118–122 (1982). doi:10.1016/0370-2693(82)90988-1
7. J. Su, L. Zhu, W.J. Xie, F.S. Zhang, Nuclear temperatures from kinetic characteristics. *Phys. Rev. C* **85**, 017604 (2012). doi:10.1103/PhysRevC.85.017604
8. W. Trautmann et al., Thermal and chemical freeze-out in spectator fragmentation. *Phys. Rev. C* **76**, 064606 (2007). doi:10.1103/PhysRevC.76.064606
9. C.-W. Ma, S.-S. Wang, J. Pu et al., Temperature of heavy fragments in heavy-ion collisions. *Commun. Theor. Phys.* **59**, 95–98 (2013). doi:10.1088/0253-6102/59/1/17
10. C. Ma, C. Qiao, S. Wang et al., Temperature and symmetry energy of neutron-rich fragments in the 1A GeV  $^{124,136}\text{Xe} + \text{Pb}$  reactions. *Nucl. Sci. Tech.* **24**, 050510 (2013). URL:www.j.sinap.ac.cn/nst/CN/Y2013/V24/I5/50510
11. C.W. Ma, J. Pu, Y.G. Ma et al., Temperature determined by isobaric yield ratios in heavy-ion collisions. *Phys. Rev. C* **86**, 054611 (2012). doi:10.1103/PhysRevC.86.054611
12. C.W. Ma, X.L. Zhao, J. Pu et al., Temperature determined by isobaric yield ratios in a grand-canonical ensemble theory. *Phys. Rev. C* **88**, 014609 (2013). doi:10.1103/PhysRevC.88.014609
13. M. Yu, H.L. Wei, C.W. Ma, Probing temperature from intermediate mass fragment by isobaric yield ratio in heavy-ion collisions. *Commun. Theor. Phys.* **64**, 727–730 (2015). doi:10.1088/0253-6102/64/6/727
14. C.W. Ma, T.T. Ding, C.Y. Qiao, X.G. Cao, Improved thermometer for intermediate-mass fragments in heavy-ion collisions with isobaric yield ratio difference. *Phys. Rev. C* **92**, 064601 (2015). doi:10.1103/PhysRevC.92.064601
15. X. Liu, W. Lin, R. Wada et al., Primary isotope yields and characteristic properties of the fragmenting source in heavy-ion reactions near the Fermi energy. *Phys. Rev. C* **90**, 014605 (2014). doi:10.1103/PhysRevC.90.014605
16. X. Liu, W. Lin, M. Huang et al., Freezeout concept and dynamical transport model in intermediate-energy heavy-ion reactions. *Phys. Rev. C* **92**, 014623 (2015). doi:10.1103/PhysRevC.92.014623
17. X. Liu, M. Huang, R. Wada et al., Symmetry energy extraction from primary fragments in intermediate heavy-ion collisions. *Nucl. Sci. Tech.* **26**, S20508 (2015). doi:10.13538/j.1001-8042/nst.26.S20508
18. M. Huang, Z. Chen, S. Kowalski et al., Isobaric yield ratios and the symmetry energy in heavy-ion reactions near the Fermi energy. *Phys. Rev. C* **81**, 044620 (2010). doi:10.1103/PhysRevC.81.044620
19. C.W. Ma, J. Pu, H.L. Wei et al., Symmetry energy extracted from fragments in relativistic energy heavy-ion collisions induced by  $^{124,136}\text{Xe}$ . *Eur. Phys. J. A* **48**, 78 (2012). doi:10.1140/epja/i2012-12078-5
20. C.W. Ma, J. Pu, S.S. Wang et al., The Symmetry Energy from the Neutron-Rich Nucleus Produced in the Intermediate-Energy  $^{40,48}\text{Ca}$  and  $^{58,64}\text{Ni}$  Projectile Fragmentation. *Chin. Phys. Lett.* **29**, 062101 (2012). doi:10.1088/0256-307X/29/6/062101
21. C.W. Ma, H.L. Song, J. Pu et al., Symmetry energy from neutron-rich fragments in heavy-ion collisions, and its dependence on incident energy, and impact parameters. *Chin. Phys. C* **37**, 024102 (2013). doi:10.1088/1674-1137/37/2/024102
22. C.W. Ma, S.S. Wang, Y.L. Zhang et al., Residue Coulomb interaction among isobars and its influence in symmetry energy of neutron-rich fragment. *Commun. Theor. Phys.* **64**, 334–340 (2015). doi:10.1088/0253-6102/64/3/334
23. B.A. Li, C.M. Ko, Isospin relaxation time in heavy-ion collisions at intermediate energies. *Phys. Rev. C* **57**, 2065 (1998). doi:10.1103/PhysRevC.57.2065
24. J. Decharge, D. Gogny, Hartree-Fock-Bogolyubov calculations with the D1 effective interaction on spherical nuclei. *Phys. Rev. C* **21**, 1568 (1980). doi:10.1103/PhysRevC.21.1568
25. A. Ono, P. Danielewicz, W.A. Friedman et al., Isospin fractionation and isoscaling in dynamical simulations of nuclear collisions. *Phys. Rev. C* **68**, 051601(R) (2003). doi:10.1103/PhysRevC.68.051601

26. R.W. Minich, S. Agarwal, A. Bujak et al., Critical phenomena in hadronic matter and experimental isotopic yields in high energy proton-nucleus collisions. *Phys. Lett. B* **118**, 458 (1982). doi:[10.1016/0370-2693\(82\)90224-6](https://doi.org/10.1016/0370-2693(82)90224-6)
27. C.W. Ma, J.B. Yang, M. Yu et al., Surface and volume symmetry energy coefficients of a neutron-rich nucleus. *Chin. Phys. Lett.* **29**, 092101 (2012). doi:[10.1088/0256-307x/29/9/092101](https://doi.org/10.1088/0256-307x/29/9/092101)
28. M. Wang, G. Audi, A.H. Wapstra et al., The Ame2012 atomic mass evaluation. *Chin. Phys. C* **36**, 1603 (2012). doi:[10.1088/1674-1137/36/12/003](https://doi.org/10.1088/1674-1137/36/12/003)
29. S.J. Lee, A.Z. Mekjian, Symmetry and surface symmetry energies in finite nuclei. *Phys. Rev. C* **82**, 064319 (2010). doi:[10.1103/PhysRevC.82.064319](https://doi.org/10.1103/PhysRevC.82.064319)
30. C.W. Ma, H.L. Wei, S.S. Wang et al., Isobaric yield ratio difference and Shannon information entropy. *Phys. Lett. B* **742**, 19–22 (2015). doi:[10.1016/j.physletb.2015.01.015](https://doi.org/10.1016/j.physletb.2015.01.015)
31. C.W. Ma, Y.D. Song, C.Y. Qiao et al., A scaling phenomenon in the difference of Shannon information uncertainty of fragments in heavy-ion collisions. *J. Phys. G: Nucl. Part. Phys.* **43**, 045102 (2016). doi:[10.1088/0954-3899/43/4/045102](https://doi.org/10.1088/0954-3899/43/4/045102)